

# **Chapter 1**

## Introduction and Summary

## Photocatalysis

Semiconductor photocatalysis has received much attention during last three decades as a promising solution for both energy generation and environmental problems. Since the discovering of Fujishima and Honda<sup>1</sup> that water can be photo-electrochemically decomposed into hydrogen and oxygen using a semiconductor (TiO<sub>2</sub>) electrode under UV irradiation, extensive works have been carried out to produce hydrogen from water splitting using a variety of semiconductor photocatalysts. In recent years, scientific and engineering interest in heterogeneous photocatalysis has been also focused on environmental applications such as water treatment and air purification. Many review papers on semiconductor photocatalysis can be found in literature.<sup>2-6</sup>

Semiconductor photocatalysis is initiated by electron-hole pairs after bandgap excitation. When a photocatalyst is illuminated by light with energy equal to or greater than band-gap energy, the valence band electrons can be excited to the conduction band, leaving a positive hole in the valence band:



The excited electron-hole pairs can recombine, releasing the input energy as heat, with no chemical effect. However, if the electrons (and holes) migrate to the surface of the semiconductor without recombination, they can participate in various oxidation and reduction reactions with adsorbed species such as water, oxygen, and other organic or inorganic species. These oxidation and reduction reactions are the basic mechanisms of photocatalytic water/air remediation and photocatalytic hydrogen production, respectively. A simplified mechanism for photocatalytic process on a semiconductor is presented in Figure 1.1.

For photocatalytic water/air remediation as an environmental application, valence band (VB) holes are the important elements that induce the oxidative decomposition of environmental pollutants. The positive hole can oxidize pollutants directly, but mostly they react with water (i.e., hydroxide ion,  $\text{OH}^-$ ) to produce the hydroxyl radical ( $\bullet\text{OH}$ ), which is the very powerful oxidant with the oxidation potential of 2.8 V (NHE).  $\bullet\text{OH}$  rapidly attacks pollutants at the surface and in solution as well and can mineralize them into  $\text{CO}_2$ ,  $\text{H}_2\text{O}$ , etc.  $\text{TiO}_2$ , the most popular photocatalyst because of its relatively high activity, chemical stability, availability with low production costs, and non-toxicity has been widely studied and proven to have a potential to completely oxidize a variety of organic compounds, including persistent organic pollutants.

The reducing conduction band (CB) electrons are more important when photocatalytic reaction is applied for hydrogen production from water splitting. In order to initiate hydrogen production, the conduction band level must be more negative than the hydrogen production level:



The redox potential for overall reaction (eq. 1.2) at pH 7 is  $E_{\text{H}} = -1.23$  V (NHE), with the corresponding half-reactions of  $-0.41$  V (eq 1.4) and  $0.82$  V (eq 1.5), which gives a  $\Delta G^\circ = +237$  kJ/mole).<sup>7</sup>

A large number of metal oxides and sulfides have been examined as photocatalysts for hydrogen production and environmental application. The majority of the simple metal

oxide photocatalysts, however, are primarily active under UV irradiation ( $\lambda < 385$  nm or  $E_{\text{bg}} \geq 3.0$  eV), present in only a small portion of solar light (Table 1.1). For example,  $\text{TiO}_2$  has a wide band-gap energy of  $3.0 \sim 3.2$  eV which prevents the utilization of visible-light that accounts for most of solar energy. More recently, significant efforts have also been made to develop new or modified semiconductor photocatalysts that are capable of using visible-light ( $\lambda = 400\text{--}700$  nm) including metal ion doping, nonmetallic element doping, and sensitization with organic dyes or small band-gap semiconductors such as CdS.

Metal ion doping has been primarily studied to enhance the photocatalytic activity under UV irradiation. In recent years, however, extensive research works have focused on visible-light induced photocatalysis by metal ion-doped semiconductor, since some of these have shown the extended absorption spectra into visible-light region. This property has been explained by the excitation of electrons of dopant ion to the conduction band of semiconductor (i.e., a metal to conduction band charge-transfer). Numerous metal ions, including transition metal ions (e.g., vanadium, chromium, iron, nickel, cobalt, ruthenium and platinum) and rare earth metal ions (e.g., lanthanum, cerium, and ytterbium), have been investigated as potential dopants for visible-light induced photocatalysis. However, metal ion dopant can also serve as a recombination center, resulting in decreased photocatalytic activities.

The studies of visible-light active semiconductors doped with nonmetallic elements such as nitrogen (N), sulfur (S), and carbon (C) have been intensively carried out since the study of N-doped  $\text{TiO}_2$  by Asahi and coworkers in 2001.<sup>8</sup> It was originally proposed that N doping of  $\text{TiO}_2$  can shift its photo-response into the visible region by mixing of p

states of nitrogen with 2p states of lattice oxygen and increase photocatalytic activity by narrowing the  $\text{TiO}_2$  band-gap. However, more recent studies have shown both theoretically and experimentally that the nitrogen species result in localized N 2p states above the valence band and the electronic transitions from localized N 2p state to the CB are made in  $\text{TiO}_2$  under visible-light irradiation.<sup>9-11</sup> Unlike metal ion doping, nonmetallic dopants replace lattice oxygen and are less likely form recombination centers.

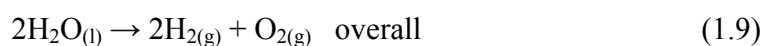
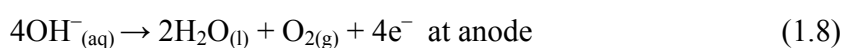
Sensitization methods are widely used to utilize visible-light for energy conversion. In case of sensitization with organic dyes, dye molecule electrons excited by visible light can be injected to the CB of semiconductor to initiate the catalytic reactions as shown in Figure 1.2(a). Similarly, sensitization with a small band-gap semiconductor is made by coupling a large band-gap semiconductor with a small band-gap semiconductor with a more negative conduction level (i.e., hybrid or composite photocatalyst). In composite photocatalyst, the CB electrons photo-generated from a small band-gap semiconductor by the absorption of visible-light can be injected to the CB of a large band gap semiconductor, while the photo-generated holes are trapped in a small band-gap semiconductor. Thus, an effective electron-hole separation can be achieved, as shown in Figure 1.2(b). CdS with band-gap energy of 2.4 eV has been frequently used to form hybrid or composite photocatalysts.

## **Electrolysis**

Water electrolysis is considered the easiest and cleanest method to produce a large quantity of hydrogen without carbon emission when the required electricity is derived from renewable energy resources. Water electrolysis, first demonstrated in 1800 by

Nicholson et al., has grown in a variety of industrial markets in recent years.<sup>12</sup> Two electrolyzer technologies, alkaline and proton exchange membrane (PEM), currently exist at the commercial level with solid oxide electrolysis in the research phase.<sup>13</sup> Nowadays the research has focused on development of a high efficiency electrolyzer. The U.S. Department of Energy (DOE) has established a target energy efficiency of 76% (corresponding to \$2.75/GGE H<sub>2</sub>) for hydrogen generation via electrolysis by 2015 from a current average energy efficiency of 62%.<sup>14</sup> In addition, solar-light-driven water electrolysis integrated with photovoltaic (PV) system has been suggested and widely tested, since the primary disadvantage of water electrolysis is the high electric consumption, especially in large-scale application.

Water electrolysis is defined as splitting of water with an electric current. When a direct current (DC) is passed between two electrodes immersed in water in the presence of electrolyte, water can be decomposed to hydrogen at the negatively biased electrode (cathode) and to oxygen at the positively biased electrode (anode). The voltage applied to the cell must be greater than the free energy of formation of water plus the corresponding activation and Ohmic losses:



In addition, there has been increasing interest in development of electrochemical oxidation technology for environmental application (i.e., water and wastewater treatment) because of its advantages, including versatility, energy efficiency, amenability to

automation, and robustness. This technology has been applied to the electrochemical degradation of various environmental organic contaminants such as dyes, phenols, surfactants, herbicides, and endocrine-disrupting chemicals, and (more recently) for the treatment of domestic wastewater, industrial wastewater and landfill leachate. The electrochemical oxidation of environmental organic contaminants can occur via direct oxidation on the anode surface or indirect oxidation mediated by electro-generated oxidants such as  $\text{OH}\cdot$  radicals, ozone,  $\text{H}_2\text{O}_2$ , and active chlorine species ( $\text{Cl}\cdot$ ,  $\text{Cl}_2\cdot^-$ , and  $\text{OCl}^-$ ) in the presence of chloride ions.

## **Thesis Overview and Summary**

This thesis consists of 7 chapters. Chapter 1 (this chapter) describes the general background of photocatalysis and electrolysis. Chapter 2 through Chapter 6 are research works for the development of visible-light active photocatalysts for environmental application and hydrogen production. Chapter 2 and Chapter 3 examine the metal ion-doped titanium dioxide ( $\text{TiO}_2$ ) photocatalysts for environmental applications, and Chapter 4 through Chapter 6 are studies of hybrid (composite) photocatalysts with cadmium sulfide ( $\text{CdS}$ ) semiconductor for hydrogen production. Finally, Chapter 7 focuses on a hybrid electrochemical system for the production of hydrogen and simultaneous degradation of organic pollutants.

Chapter 2 investigates 13 different metal ion-doped  $\text{TiO}_2$  nanoparticles synthesized by standard sol-gel method and compares the effects of individual dopants on the resulting physicochemical properties (e.g., a crystal structure and UV-vis absorption), and their corresponding photocatalytic activities with respect to the catalysis of several reactions

under visible-light irradiation. Metal ion doping results in changing anatase to rutile phase transformation (A-R phase transformation) temperature and the photophysical response of TiO<sub>2</sub>. However, the results of visible-light induced photocatalysis with metal ion-doped TiO<sub>2</sub> suggest that the presence of the rutile structure in the doped TiO<sub>2</sub> may affect photocatalytic activities of M-TiO<sub>2</sub> whereas their corresponding UV-vis absorption spectra seem to be not directly correlated with the visible-light photocatalytic activities of various metal ion-doped TiO<sub>2</sub> materials. This chapter was accepted at *Journal of Physical Chemistry C* in November 2009.

Chapter 3 examines the efficacy of double-doping with metal ions, including platinum (Pt), chromium (Cr), vanadium (V), and nickel (Ni), which are individually shown visible-light photoreactivity. The two metals co-doped TiO<sub>2</sub> materials are also prepared by standard sol-gel methods with the doping levels of 0.1 to 0.5 atom-%, and the changes of physicochemical properties induced by co-doping of two metal ions are investigated by various techniques such as XRD, BET surface-area measurement, SEM, and UV-Vis diffuse reflectance spectroscopy. Some of the co-doped TiO<sub>2</sub> nanoparticles showed the enhanced visible-light photocatalytic activities, and 0.3 atom-% Pt-Cr-TiO<sub>2</sub> and 0.3 atom-% Cr-V-TiO<sub>2</sub> showed the highest photoreactivity with respect to MB degradation and iodide oxidation, respectively. However, none of the co-doped TiO<sub>2</sub> samples have enhanced photocatalytic activity for phenol degradation when compared to their single-doped TiO<sub>2</sub> counterparts. This chapter is currently in press with the *Journal of Materials Research* for a focus issue (Energy and Environmental Sustainability) that will be published in January 2010.

Chapter 4 explores the Ni/NiO/KNbO<sub>3</sub>/CdS nanocomposite system synthesized by solid-state reactions. Their physicochemical properties and visible-light photocatalytic activity for H<sub>2</sub> production are investigated in the presence of isopropanol as an electron donor. It is shown that the inherent photocatalytic activity of bulk-phase CdS was enhanced by combining Q-sized CdS with KNbO<sub>3</sub> and Ni deposited on KNbO<sub>3</sub>, which is most likely due to effective charge separation of photogenerated electrons and holes in CdS that is achieved by electron injection into the conduction band of KNbO<sub>3</sub>, and the reduced states of niobium (e.g., Nb(IV) and Nb(III)) by mediating effective electron transfer to bound protons. We also observe that efficient attachment of Q-size CdS and the deposition of nickel on the KNbO<sub>3</sub> surface increases H<sub>2</sub> production rates. Other factors that influence H<sub>2</sub> production rate, including the nature of the electron donors and the solution pH are also determined in this chapter. This chapter was published in *Journal of Materials Chemistry* in 2008.

Chapter 5 further investigates CdS combined photocatalyst composite systems such as CdS/zeolite and CdS/potassium niobates (KNbO<sub>3</sub>) in the presence of various electron donors. The relative order of visible-light photocatalytic activity for hydrogen production is determined: Ni(0)/NiO/KNbO<sub>3</sub>/CdS > Ni(0)/KNbO<sub>3</sub>/CdS > KNbO<sub>3</sub>/CdS > CdS/NaY-Zeolite > CdS/TiY-Zeolite > CdS. The photoreactivity order with respect to the array of electron donors is 2-propanol > ethanol > methanol > sulfite > sulfide > H<sub>2</sub>O. The rates of hydrogen production from water and water-alcohol mixtures were correlated with fluorescent emission spectra and fluorescence lifetimes. In addition, the partial reduction of Cd(II) to Cd(0) on the surface of CdS in various composite systems is observed. This project is a collaboration with Dr. Su-Young Ryu and William Balcerski. I synthesized

and optimized the nanocomposites materials. This chapter is published in *Industrial & Engineering Chemistry Research* (Ryu, S.Y.; Choi, J.; Balcerski, W.; Lee, T.K.; Hoffmann, M. R. *Ind. & Eng. Chem. Res.* **2007**, *46*, 7476).

Chaper 6 examines a mixed-phase CdS matrix interlinked with elemental Pt deposits (i.e., c-CdS/Pt/hex-CdS composites) for visible-light induced photocatalytic hydrogen production. The quantum-sized cubic-phase CdS (c-CdS) with average particle diameters of 13 nm and a band-gap energy of 2.6 eV is synthesized and then coupled with hexagonal phase CdS (hex-CdS) in the bulk-phase size domain that has a band-gap energy of 2.4 eV with interlink of Pt metal deposits. Under visible-light irradiation, the resulting hybrid nanocomposites efficiently produce hydrogen in the presence of sodium sulfide and sodium sulfite at pH 14. Hydrogen production rates were very low with the same composite at pH 7 in a water-isopropanol solvent. The relative order of reactivity for the synthesized hybrid catalysts is: c-CdS/Pt/hex-CdS > Pt/c-CdS/hex-CdS > c-CdS/hex-CdS > Pt/hex-CdS > hex-CdS > quantum-sized c-CdS. This project is a collaboration with Dr. Luciana A. Silva and I participated in development of the synthetic method of hybrid materials, characterization, and discussion of results. (Silva, L.A.; Ryu, S.Y.; Choi, J.; Choi, W.; Hoffmann, M. R. *Journal of Physical Chemistry C* **2008**, *112*, 12069)

Finally Chapter 7 focuses on the hybridized electrochemical system for the production of hydrogen and simultaneous degradation of organic pollutants. Electrolytic hydrogen production is less economically viable due to its high electric energy consumption. By hybridizing electrolytic hydrogen production with water treatment, however, the electrochemical system can be more economically viable. Our group previously

introduced a hybridized electrochemical cell composed of a stainless steel cathode and a Bi-doped TiO<sub>2</sub> anode for the oxidation of phenol with simultaneous hydrogen production.<sup>15-17</sup> As a follow-on study, this chapter investigates a sub-pilot size scaled-up hybrid electrochemical system with Bi-doped TiO<sub>2</sub> anodes and SS cathodes for practical applications. This system degrades a variety of common organic pollutants such as methylene blue (MB), rhodamine B (Rh.B), phenol, and triclosan. Industrial wastewater is effectively treated as well. The kinetics of substrates oxidation are investigated as a function of the cell current, substrate concentration, and background electrolyte such as NaCl and Na<sub>2</sub>SO<sub>4</sub>; average current efficiencies were in the range of 4~22 %. The cathodic current efficiency and energy efficiency for simultaneous hydrogen production were determined to be 50~70% and 20~40 %, respectively. A solar-powered electrochemical system driven by a commercial photovoltaic (PV) panel for both wastewater treatment and hydrogen production is successfully demonstrated in this chapter.

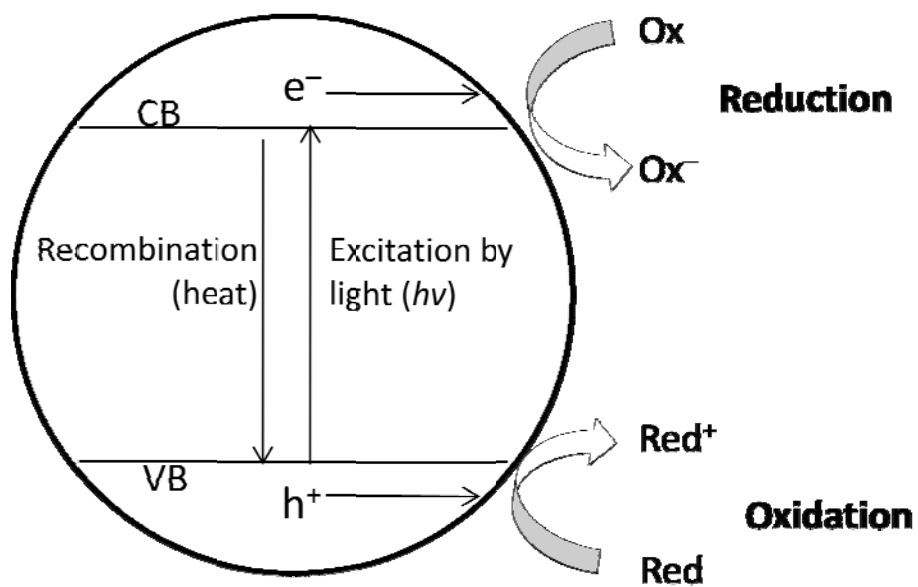


**Figure 1.1.** Simplified mechanism of semiconductor photocatalytic process

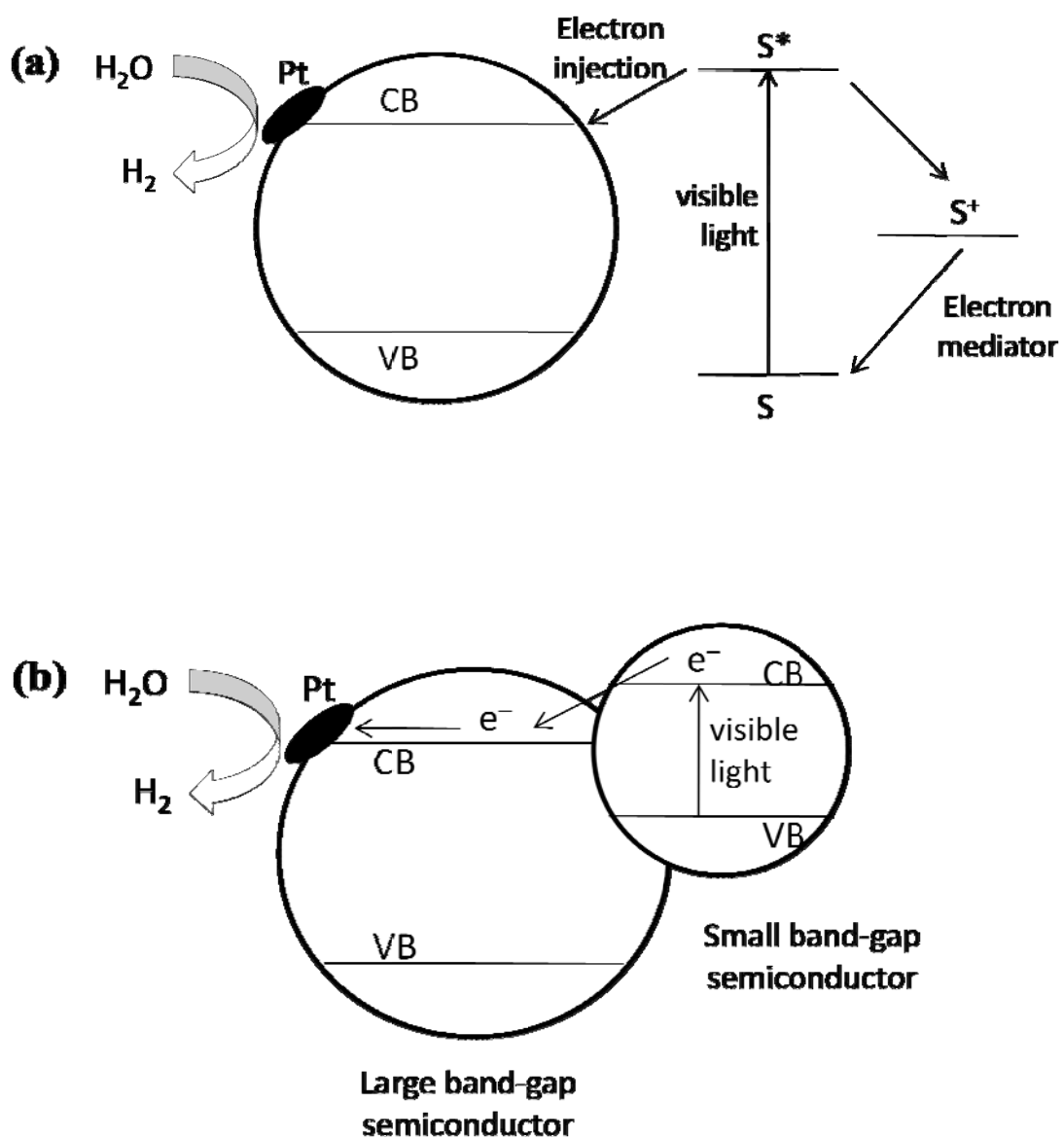


**Figure 1.2.** Schematic diagram of visible-light induced photocatalysis with sensitizations: (a) sensitization with organic dyes and (b) sensitization with small band-gap semiconductor (photocatalyst composites)

**TABLE 1.1.** Band-gap energies for several common semiconductor materials<sup>18,19</sup>

Semiconductor	Band-gap energy (eV)
Diamond	5.4
TiO <sub>2</sub>	3.0~3.2
WO <sub>3</sub>	2.7
ZnO	3.2
SnO <sub>2</sub>	3.5
SrTiO <sub>3</sub>	3.4
Fe <sub>2</sub> O <sub>3</sub>	2.2
CdS	2.4
ZnS	3.7
CdSe	1.7
GaP	2.3
GaAs	1.4
SiC	3.0

## References

- (1) Fujishima, A.; Honda, K. *Nature* **1972**, *238*, 37.
- (2) Hoffmann, M. R.; Martin, S. T.; Choi, W. Y.; Bahnemann, D. W. *Chem. Rev.* **1995**, *95*, 69.
- (3) Linsebigler, A. L.; Lu, G. Q.; Yates, J. T. *Chem. Rev.* **1995**, *95*, 735.
- (4) Mills, A.; LeHunte, S. *J. Photochem. Photobiol. A* **1997**, *108*, 1.
- (5) Zhao, J.; Yang, X. D. *Building and Environment* **2003**, *38*, 645.
- (6) Bahnemann, D. *Sol. Energ.* **2004**, *77*, 445.
- (7) Kudo, A.; Kato, H.; Tsuji, I. *Chem. Lett.* **2004**, *33*, 1534.
- (8) Asahi, R.; Morikawa, T.; Ohwaki, T.; Aoki, K.; Taga, Y. *Science* **2001**, *293*, 269.
- (9) Batzill, M.; Morales, E. H.; Diebold, U. *Phys. Rev. Lett.* **2006**, *96*,
- (10) Livraghi, S.; Paganini, M. C.; Giamello, E.; Selloni, A.; Di Valentin, C.; Pacchioni, G. *J. Am. Chem. Soc.* **2006**, *128*, 15666.
- (11) Di Valentin, C.; Pacchioni, G.; Selloni, A.; Livraghi, S.; Giamello, E. *J. Phys. Chem. B* **2005**, *109*, 11414.
- (12) <http://www.rsc.org/chemistryworld/Issues/2003/August/electrolysis.asp>
- (13) *Solar Hydrogen Generation: Toward a Renewable Energy Future*; Springer: New York, 2008.
- (14) *Solar and Wind Technologies for Hydrogen Production*, (available at [http://www.hydrogen.energy.gov/congress\\_reports.html](http://www.hydrogen.energy.gov/congress_reports.html).)
- (15) Park, H.; Vecitis, C. D.; Choi, W.; Weres, O.; Hoffmann, M. R. *J. Phys. Chem. C* **2008**, *112*, 885.
- (16) Park, H.; Vecitis, C. D.; Hoffmann, M. R. *J. Phys. Chem. A* **2008**, *112*, 7616.
- (17) Park, H.; Vecitis, C. D.; Hoffmann, M. R. *J. Phys. Chem. C* **2009**, *113*, 7935.

- (18) Bhatkhande, D. S.; Sawant, S. B.; Schouten, J. C.; Pangarkar, V. G. *J. Chem. Technol. Biotechnol.* **2004**, *79*, 354.
- (19) Gratzel, M. *Nature* **2001**, *414*, 338.